

AXIAL QUADRUPOLE AND OCTUPOLE DYNAMICS IN HEAVY EVEN-EVEN NUCLEI

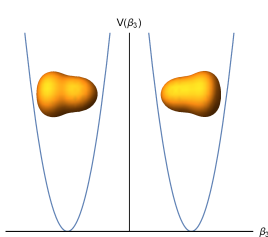
Radu Budaca

IFIN-HH, Măgurele, România

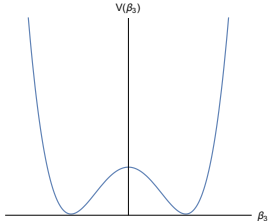
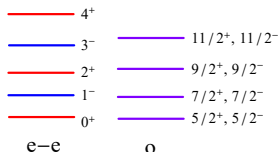


P. Buganu
A. I. Budaca

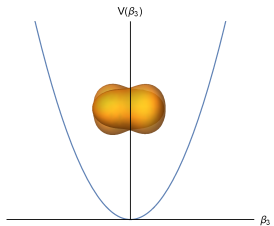
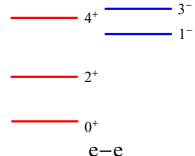
Dynamics of octupole deformation and its spectral signatures



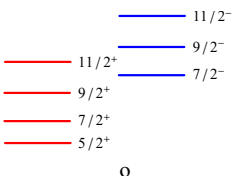
Static (rigid) β_3



intermediary dynamical
regime (tunneling)



Dynamic β_3 (oscillations)



- Enhanced $E1$ and $E3$ transitions.

Quadrupole-octupole collective Hamiltonian

Quadrupole ($\beta_2 = \alpha_{20}$) and octupole ($\beta_3 = \alpha_{30}$) deformation variables limited to axial symmetry \Rightarrow

$$H = - \sum_{\lambda=2,3} \frac{\hbar^2}{2B_\lambda} \frac{1}{\beta_\lambda^3} \frac{\partial}{\partial \beta_\lambda} \beta_\lambda^3 \frac{\partial}{\partial \beta_\lambda} + \frac{\hbar^2 \hat{L}^2}{6(B_2 \beta_2^2 + 2B_3 \beta_3^2)} + U(\beta_2, \beta_3)$$

Solutions $\Phi_{LMK}^\pm(\beta_2, \beta_3, \theta) = (\beta_2 \beta_3)^{-3/2} \Psi_L^\pm(\beta_2, \beta_3) |LMK, \pm\rangle$.

Notations: $\tilde{\beta}_2 = \beta_2 \sqrt{\frac{B_2}{B}}$, $\tilde{\beta}_3 = \beta_3 \sqrt{\frac{B_3}{B}}$, $B = \frac{B_2 + B_3}{2}$, $\epsilon = \frac{2B}{\hbar^2} E$, $u = \frac{2B}{\hbar^2} U$

Change of variables: $\tilde{\beta}_2 = \tilde{\beta} \cos \phi$, $\tilde{\beta}_3 = \tilde{\beta} \sin \phi$, $\tilde{\beta} = \sqrt{\tilde{\beta}_2^2 + \tilde{\beta}_3^2}$

$$\phi = \begin{cases} 0, & \text{Pure quadrupole deformation } (\beta_3 = 0) \\ \pm\pi/2, & \text{Pure octupole deformation } (\beta_2 = 0) \end{cases}$$

\Downarrow Integration over Euler angles θ for $K = 0$

$$\left[-\frac{\partial^2}{\partial \tilde{\beta}^2} - \frac{1}{\tilde{\beta}} \frac{\partial}{\partial \tilde{\beta}} + \frac{L(L+1)}{3\tilde{\beta}^2(1+\sin^2 \phi)} - \frac{1}{\tilde{\beta}^2} \frac{\partial^2}{\partial \phi^2} + u(\tilde{\beta}, \phi) + \frac{3}{\tilde{\beta}^2 \sin^2 2\phi} - \epsilon_L \right] \Psi_L^\pm(\tilde{\beta}, \phi) = 0$$

[V. Yu. Denisov, A. Ya. Dzyublik, Nucl. Phys. A 589 (1995) 17]



- Separable potential $u(\tilde{\beta}, \phi) = u(\tilde{\beta}) + u(\phi)/\tilde{\beta}^2$.
- Factorized wave-function $\Psi_L^\pm(\tilde{\beta}, \phi) = \psi_L^\pm(\tilde{\beta})\chi_L^\pm(\phi)$.
- Separation constant W_L^\pm

Radial-like equation:

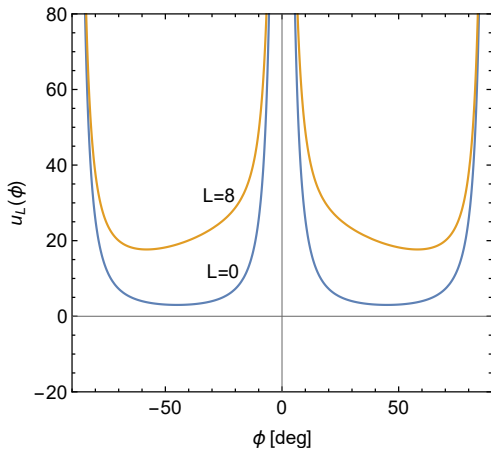
$$\left[-\frac{\partial^2}{\partial \tilde{\beta}^2} - \frac{1}{\tilde{\beta}} \frac{\partial}{\partial \tilde{\beta}} + \frac{W_L^\pm}{\tilde{\beta}^2} + u(\tilde{\beta}) \right] \psi_L^\pm(\tilde{\beta}) = \epsilon_L \psi_L^\pm(\tilde{\beta}),$$

Angular equation:

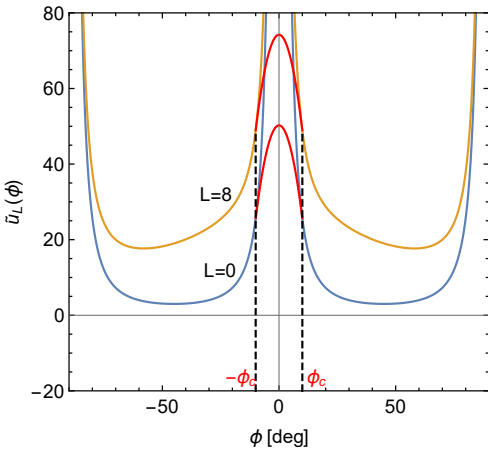
$$\left[-\frac{\partial^2}{\partial \phi^2} + u(\phi) + u_L(\phi) \right] \chi_L^\pm(\phi) = W_L^\pm \chi_L^\pm(\phi),$$

where

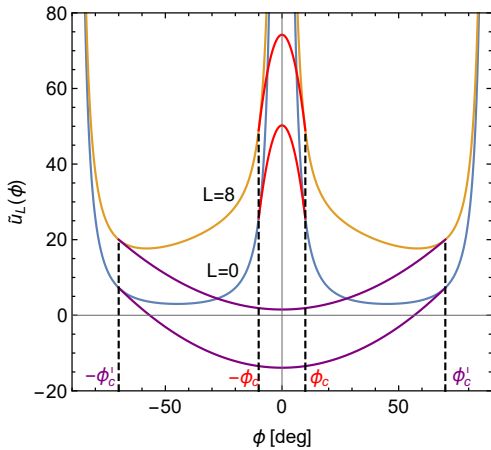
$$u_L(\phi) = \frac{3}{\sin^2 2\phi} + \frac{L(L+1)}{3(1+\sin^2 \phi)}.$$



$$u_L(\phi) = \frac{3}{\sin^2 2\phi} + \frac{L(L+1)}{3(1 + \sin^2 \phi)}$$



$$u_L(\phi) = \frac{3}{\sin^2 2\phi} + \frac{L(L+1)}{3(1+\sin^2 \phi)} \quad v(\phi) = -a\phi^2 + b$$



$$u_L(\phi) = \frac{3}{\sin^2 2\phi} + \frac{L(L+1)}{3(1+\sin^2 \phi)} \quad v(\phi) = -a\phi^2 + b$$

Parameters a and b are determined from the continuity condition at ϕ_c :

$$u_L(\phi_c) = v(\phi_c), \quad \left. \frac{\partial u_L(\phi)}{\partial \phi} \right|_{\phi_c} = \left. \frac{\partial v(\phi)}{\partial \phi} \right|_{\phi_c},$$

The modified potential: $\tilde{u}_L(\phi) = \begin{cases} v_L(\phi), & |\phi| < \phi_c, \\ u_L(\phi), & |\phi| \geq \phi_c, \end{cases}$

ϕ equation is diagonalized in the basis:

$$f_n^+(\phi) = \sqrt{\frac{2}{\pi}} \cos (2n - 1)\phi,$$

$$f_n^-(\phi) = \sqrt{\frac{2}{\pi}} \sin 2n\phi.$$

$u(\phi) = w_0 = \text{const.}$ - compensating parameter for $(W_L^\pm > 0)$

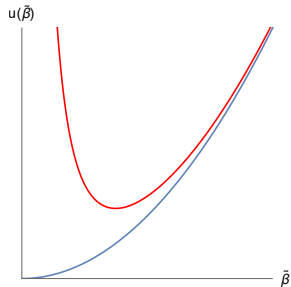
$\tilde{\beta}$ equation - harmonic oscillator

Harmonic oscillator potential:

$$u(\tilde{\beta}) = \tilde{\beta}^2$$

Energy

$$E_{Ln}^{\pm} = \frac{\hbar^2}{2B} \epsilon_{Ln} = \frac{\hbar^2}{B} (2n + \nu_L^{\pm} + 1)$$



Wave-function:

$$\psi_{Ln}^{\pm}(\tilde{\beta}) = \sqrt{\frac{2n!}{\Gamma(n + \nu_L^{\pm} + 1)}} \tilde{\beta}^{\nu_L^{\pm}} L_n^{\nu_L^{\pm}}(\tilde{\beta}^2) e^{-\tilde{\beta}^2/2}$$

$$\nu_L^{\pm} = \sqrt{W_L^{\pm} + w_0}, \quad n = 0, 1, 2, \dots$$

$n = 0$ - ground state band of \pm parity.

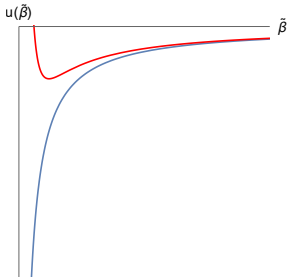
$\tilde{\beta}$ equation - hyperbolic potential

Hyperbolic potential (Coulomb):

$$u(\tilde{\beta}) = -\frac{1}{\tilde{\beta}}$$

Energy

$$E_{L_n}^{\pm} = -\frac{\hbar^2 (\eta_L^{\pm})^2}{2B} = -\frac{\hbar^2}{8B} \frac{1}{(\nu_L^{\pm} + \frac{1}{2} + n)^2}$$



Wave-function:

$$\psi_{L_n}^{\pm}(\tilde{\beta}) = (2\eta_L^{\pm})^{\nu_L^{\pm}+1} \sqrt{\frac{n!}{\Gamma(n+2\nu_L^{\pm}+1)(2n+2\nu_L^{\pm}+1)}} e^{-\eta_L^{\pm}\tilde{\beta}} \tilde{\beta}^{\nu_L^{\pm}} L_n^{2\nu_L^{\pm}} (2\eta_L^{\pm}\tilde{\beta})$$
$$\nu_L^{\pm} = \sqrt{W_L^{\pm} + w_0}, \quad n = 0, 1, 2, \dots$$

$n = 0$ - ground state band of \pm parity.

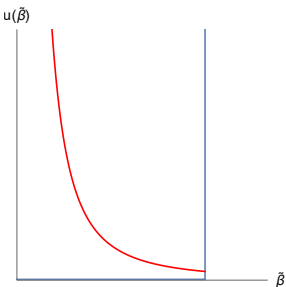
$\tilde{\beta}$ equation - infinite square well

Infinite square well potential:

$$u(\tilde{\beta}) = \begin{cases} 0, & \tilde{\beta} \leq 1 \\ \infty, & \tilde{\beta} > 1, \end{cases}$$

Energy

$$E_{Ln}^{\pm} = \frac{\hbar^2}{2B} \left[x_{n\nu_L^{\pm}} \right]^2$$



Wave-function:

$$\psi_{Ln}^{\pm}(\tilde{\beta}) = \sqrt{2} \frac{J_{\nu_L^{\pm}}(x_{n\nu_L^{\pm}} \tilde{\beta})}{J_{\nu_L^{\pm} + 1}(x_{n\nu_L^{\pm}})}$$

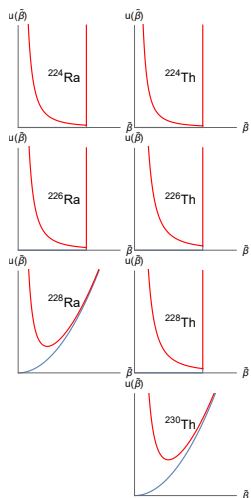
$$\nu_L^{\pm} = \sqrt{W_L^{\pm} + w_0}, \quad n = 0, 1, 2, \dots$$

$n = 0$ - ground state band of \pm parity.

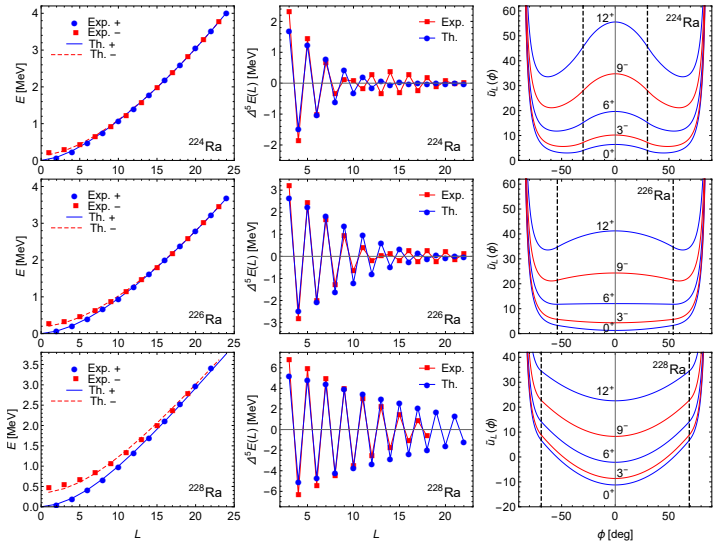
Numerical applications

$$\sigma = \sqrt{\frac{1}{N} \sum_{states}^N \left(\frac{E_{exp}(L^\pm)}{E_{exp}(2^+)} - \frac{E_{L0}^\pm - E_{00}^+}{E_{20}^+ - E_{00}^+} \right)^2}$$

Nucl.	L_{max}^+ $/L_{max}^-$	pot.	$ \phi_c $	L_c^p	w_0	σ	$E_{exp}(2^+)$ [keV]
^{224}Ra	$24^+/23^-$	ISW	30°	0^+	-1.491	0.188	84.37
^{226}Ra	$24^+/23^-$	ISW	54°	1^-	2.137	0.187	67.67
^{228}Ra	$22^+/19^-$	HO	69°	22^+	34.468	0.572	63.82
^{224}Th	$18^+/17^-$	ISW	29°	0^+	-2.851	0.223	98.10
^{226}Th	$20^+/19^-$	ISW	45°	6^+	4.147	0.169	72.20
^{228}Th	$22^+/19^-$	ISW	65°	15^-	10.129	0.375	57.77
^{230}Th	$24^+/21^-$	HO	72.6°	$> 24^+$	68.702	0.747	53.20
^{232}Th	$24^+/23^-$	HO	78.2°	$> 24^+$	141.177	0.519	49.37
^{234}Th	$24^+/23-^*$	HO	75.9°	$> 24^+$	111.429	0.556	49.55
^{230}U	$22^+/17^-$	HO	70.2°	24^+	64.324	0.292	51.73
^{232}U	$24^+/21^-$	HO	76.8°	$> 24^+$	123.407	0.203	47.60
^{234}U	$24^+/11^-$	HO	80.5°	$> 24^+$	260.121	0.189	43.50
^{236}U	$24^+/19^-$	HO	78.6°	$> 24^+$	179.246	0.358	45.24
^{238}U	$24^+/23^-$	HO	77.9°	$> 24^+$	155.626	0.764	44.92
^{240}U	$24^+/21-^*$	HO	79.1°	$> 24^+$	198.176	0.814	45.00
^{236}Pu	$16^+/5^-$	HO	79.3°	$> 24^+$	210.496	0.064	44.63
^{238}Pu	$24^+/23^-$	HO	76.7°	$> 24^+$	165.180	0.897	44.07
^{240}Pu	$24^+/23^-$	HO	76.5°	$> 24^+$	148.866	1.068	42.82

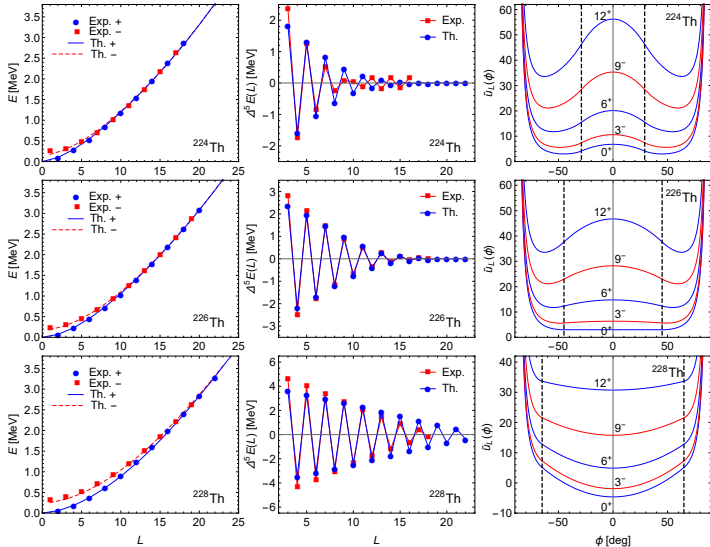


Numerical applications - energy levels



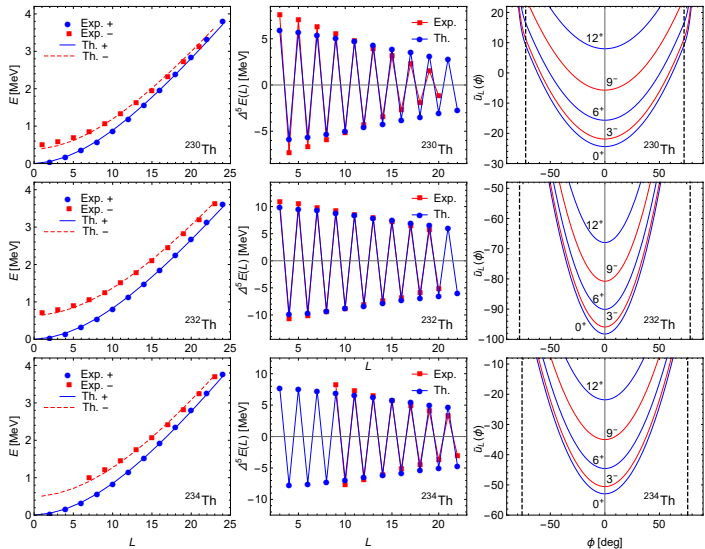
$$\begin{aligned} \Delta^5 E(L) &= 6\Delta E(L) - 4\Delta E(L-1) - 4\Delta E(L+1) + \Delta E(L+2) + \Delta E(L-2) \\ \Delta E(L) &= E(L) - E(L-1) \end{aligned}$$

Numerical applications - energy levels



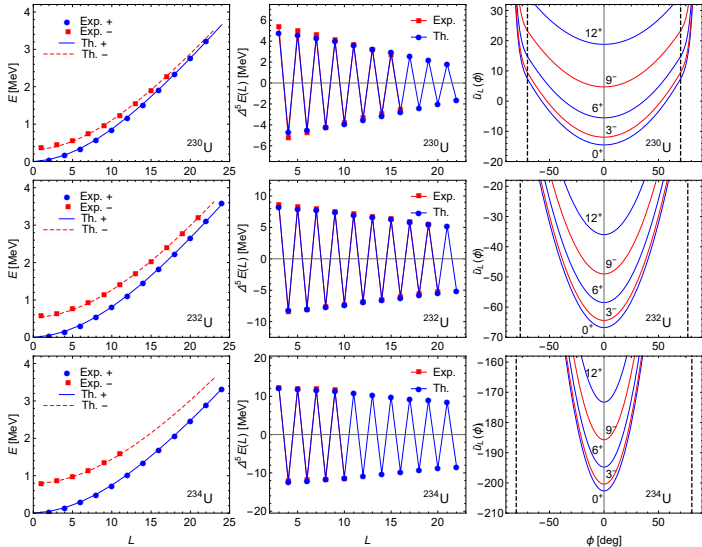
$$\begin{aligned} \Delta^5 E(L) &= 6\Delta E(L) - 4\Delta E(L-1) - 4\Delta E(L+1) + \Delta E(L+2) + \Delta E(L-2) \\ \Delta E(L) &= E(L) - E(L-1) \end{aligned}$$

Numerical applications - energy levels



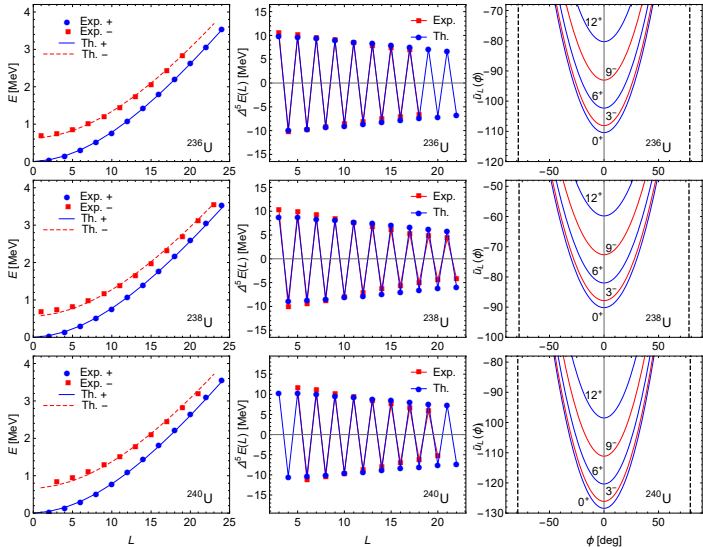
$$\begin{aligned} \Delta^5 E(L) &= 6\Delta E(L) - 4\Delta E(L-1) - 4\Delta E(L+1) + \Delta E(L+2) + \Delta E(L-2) \\ \Delta E(L) &= E(L) - E(L-1) \end{aligned}$$

Numerical applications - energy levels



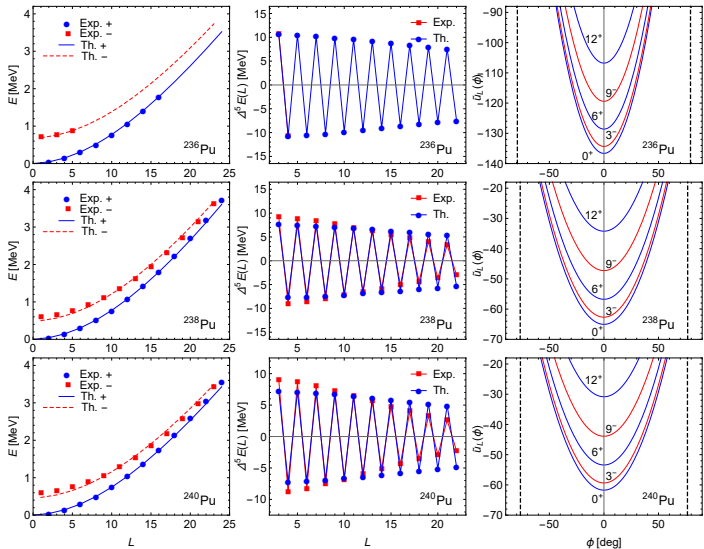
$$\begin{aligned} \Delta^5 E(L) &= 6\Delta E(L) - 4\Delta E(L-1) - 4\Delta E(L+1) + \Delta E(L+2) + \Delta E(L-2) \\ \Delta E(L) &= E(L) - E(L-1) \end{aligned}$$

Numerical applications - energy levels



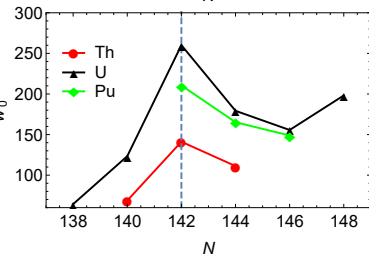
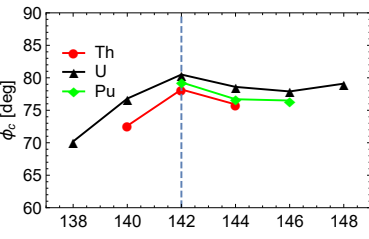
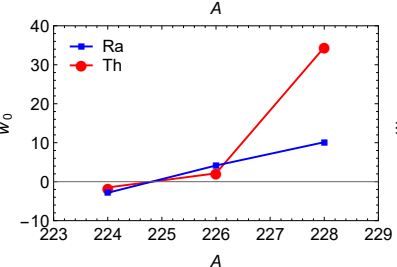
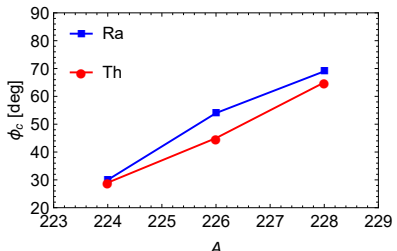
$$\begin{aligned} \Delta^5 E(L) &= 6\Delta E(L) - 4\Delta E(L-1) - 4\Delta E(L+1) + \Delta E(L+2) + \Delta E(L-2) \\ \Delta E(L) &= E(L) - E(L-1) \end{aligned}$$

Numerical applications - energy levels



$$\begin{aligned} \Delta^5 E(L) &= 6\Delta E(L) - 4\Delta E(L-1) - 4\Delta E(L+1) + \Delta E(L+2) + \Delta E(L-2) \\ \Delta E(L) &= E(L) - E(L-1) \end{aligned}$$

Numerical applications - parameters evolution



Numerical applications - excited bands

Nucleus	$E_{th}(0_2^+)$ [keV]	$E_{exp}(0_{i>1}^+)$ [keV]	$E_{th}(1_2^-)$ [keV]	$E_{exp}(1_{i>1}^-, K=0)$ [keV]
^{224}Ra	802.6	916.4	1067.3	1053.0
^{226}Ra	755.6	824.6	1099.9	1077.2
^{228}Ra	1047.6	721.2 1042.0	1405.2	
^{224}Th	803.6		1105.5	
^{226}Th	969.7	805.2	1274.3	
^{228}Th	892.2	831.8	1307.0	

Transition probabilities

$$B(E\lambda; Lnp \rightarrow L'n'p') = t_\lambda \left(C_{000}^{L\lambda L'} \right)^2 \left(\tilde{B}_{Lnp; L'n'p'}^\lambda I_{Lp; L'p'}^\lambda \right)^2$$

$\lambda = 1, 2, 3$ - multipolarity.

t_λ - gathers physical units and normalization factors.

$C_{000}^{L\lambda L'}$ - Clebsch-Gordan coefficients.

$E1 (\lambda = 1)$

$$\tilde{B}^\lambda = \int_0^\infty \tilde{\beta}^3 \psi_{Ln}^p(\tilde{\beta}) \psi_{L'n'}^{p'}(\tilde{\beta}) d\tilde{\beta}$$

$$I^\lambda = \int_{-\pi/2}^{\pi/2} \sin 2\phi \chi_L^p(\phi) \chi_{L'}^{p'}(\phi) d\phi$$

$E2 (\lambda = 2)$

$$\int_0^\infty \tilde{\beta}^2 \psi_{Ln}^p(\tilde{\beta}) \psi_{L'n'}^{p'}(\tilde{\beta}) d\tilde{\beta}$$

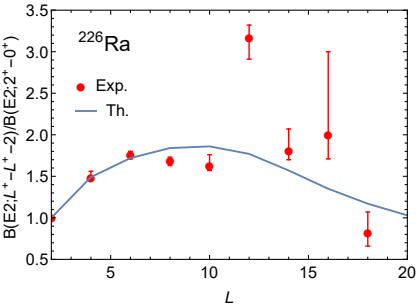
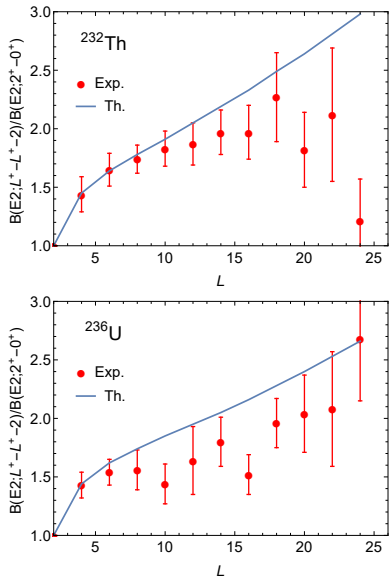
$$\int_{-\pi/2}^{\pi/2} \cos \phi \chi_L^p(\phi) \chi_{L'}^{p'}(\phi) d\phi$$

$E3 (\lambda = 3)$

$$\int_0^\infty \tilde{\beta}^2 \psi_{Ln}^p(\tilde{\beta}) \psi_{L'n'}^{p'}(\tilde{\beta}) d\tilde{\beta}$$

$$\int_{-\pi/2}^{\pi/2} \sin \phi \chi_L^p(\phi) \chi_{L'}^{p'}(\phi) d\phi$$

Numerical applications - $E2$ transitions



- $B(E1)$ transition probabilities

$$\frac{B(E1; L^- \rightarrow (L+1)^+)}{B(E1; L^- \rightarrow (L-1)^+)} > 1$$

- $B(E3)$ transition probabilities



$$\frac{B(E3; 1^- \rightarrow 2^+)}{B(E3; 3^- \rightarrow 0^+)} = \begin{cases} 5(1) \text{ Exp.} \\ 3.21 \text{ Th.} \end{cases}$$

$$\frac{B(E3; 5^- \rightarrow 2^+)}{B(E3; 3^- \rightarrow 0^+)} = \begin{cases} 1.45(42) \text{ Exp.} \\ 1.68 \text{ Th.} \end{cases}$$

$$\frac{B(E3; 0^+ \rightarrow 3^-)}{B(E3; 1^- \rightarrow 4^+)} = \begin{cases} 2.58(51) \text{ Exp.} \\ 1.71 \text{ Th.} \end{cases}$$

[L. Gaffney *et al.*, Nature **497** (2013) 199]

[NDS; F. K. McGowan *et al.*, Phys. Rev. C **10** (1974) 1146]

- An axially symmetric Bohr model is constructed for the quadrupole-octupole interaction, which is managed by an angular variable and whose spin dependence is naturally extracted from the geometry of the nuclear shape.
- Numerical applications on alternate parity bands of Ra, Th, U, and Pu nuclei, demonstrated the model's ability to describe the evolution of the octupole deformation along an isotopic chain as well as a function of spin within a rotational band.
- Ra and Th nuclei with $A = 224, 226, 228$ were identified as being part of a critical region for the transition between stable and dynamical (vibration) octupole deformation.
- The octupole transition commences at different angular momentum and is accompanied by a stabilization of quadrupole deformation.
- The model's performance is also extended to U and Pu nuclei with strong octupole vibrations.
- The distinctive trend predicted for the $E2$ transition rates in critical nuclei needs a firmer experimental confirmation.

Nuclear collective motion of heavy nuclei with axial quadrupole and octupole deformationR. Budaca^{1,2,*}, P. Buganu,¹ and A. I. Budaca¹¹ "Horia Hulubei" National Institute for Physics and Nuclear Engineering, Str. Reactorului 30, RO-077125, POB-MG6 Bucharest-Măgurele, Romania²Academy of Romanian Scientists, Splaiul Independenței 54, 050044, Bucharest, Romania

(Received 8 June 2022; accepted 6 July 2022; published 18 July 2022)

A quadrupole-octupole axially symmetric model is constructed for the unified description of alternate parity bands corresponding to octupole vibration or a stable deformation. The model depends on two parameters whose clear physical meaning allows a systematic description of the rotation-vibration dynamics of alternate parity bands analyzed for isotopic sequences of Ra, Th, U, and Pu nuclei. A critical point is identified in the $A = 224\text{--}228$ mass region of the Ra and Th nuclei marking different stages of the transition between static and dynamic octupole deformation. Model predictions are performed for energies of unobserved states of the yrast sequence and of the excited bands as well as for the $E1$, $E2$, and $E3$ transition rates, which reproduce the available experimental data and exhibit a specific spin dependence for the transitional nuclei.

DOI: [10.1103/PhysRevC.106.014311](https://doi.org/10.1103/PhysRevC.106.014311)